Chapter 4

Nonlinear Free Surface Flows with Gravity and Surface Tension

J.-M. Vanden-Broeck

Department of Mathematics, University College London, Gower Street, London, UK
j.vanden-broeck@ucl.ac.uk

This chapter is concerned with the computation of nonlinear free surface flows. Both the effects of surface tension and gravity are included in the dynamic boundary condition. Special attention is devoted to the singular behaviour at the points where free surfaces intersect rigid walls. Applications to bubbles rising in a fluid, flows emerging from a nozzle and cavitating flows are presented. It is shown how physical solutions are selected in the limit as the surface tension tends to zero.

1. Introduction

Free surface problems occur in many aspects of science and everyday life. They can be defined as problems whose mathematical formulation involves surfaces that have to be found as part of the solution. Such surfaces are called free surfaces. Examples of free surface problems are waves on a beach, bubbles rising in a glass of champagne, melting ice, flows pouring from a container and sails blowing in the wind. In these examples the free surface is the surface of the sea, the interface between the gas and the champagne, the surface of the ice, the boundary of the pouring flow and the surface of the sail.

In this chapter we concentrate on applications arising in fluid mechanics. We restrict our attention to steady, inviscid, irrotational and two-dimensional flows. The effects of gravity and surface tension are included in the nonlinear dynamic boundary condition.

Free surface flows fall into two main classes. The first is the class of such flows for which there are intersections between the free surface and a rigid surface. The classic example in this class is the flow due to a ship moving at the surface of a lake, which involves an intersection between the free surface and a rigid surface (i.e., the hull of the ship). Other examples are jets leaving a nozzle, bubbles attached to a wall and flows under a sluice gate. In each case there is a rigid surface (the nozzle, the obstacle, the wall or the gate) that intersects a free surface. The second class contains free surface flows for which there are no intersections between the free surface and a rigid wall. Here the classic example is the flow due to a submerged object moving below the surface of a lake. Other examples include free bubbles rising in a fluid and solitary waves. This chapter is concerned with the theory of free surface flows of the first class. We proceed in stages of increasing complexity.

Due to space limitation, some of the details are omitted. The reader is referred to the monograph "Gravity-Capillary Free Surface Flows" (Vanden-Broeck[5]) for a complete presentation, more examples and more references. Some of the missing parts are also suggested as exercises at the end of the chapter.

2. Basic Concepts

We first review some equations of fluid mechanics which will be used in this chapter. For further details see for example Batchelor [2] or Acheson.[1] All the fluids considered are assumed to be inviscid and to have constant density ρ (i.e., to be incompressible).

Conservation of momentum yields the Euler's equations

$$\frac{D\mathbf{u}}{Dt} = -\frac{1}{\rho}\nabla p + \mathbf{X}, \tag{1}$$

where $\mathbf{u}$ is the vector velocity, p is the pressure and $\mathbf{X}$ is the body force. Here

$$\frac{D}{Dt} = \frac{\partial}{\partial t} + \mathbf{u}\cdot\nabla, \tag{2}$$

is the material derivative. We assume that the body force $\mathbf{X}$ derives from a potential Ω, i.e.,

$$\mathbf{X} = -\nabla\Omega. \tag{3}$$

The flows are assumed to be irrotational. Therefore

$$\nabla \times \mathbf{u} = 0. \tag{4}$$

Relation (4) implies that we can introduce a potential function ϕ such that

$$\mathbf{u} = \nabla\phi. \tag{5}$$

Conservation of mass gives

$$\nabla \cdot \mathbf{u} = 0. \tag{6}$$

Then (5) and (6) imply the Laplace equation

$$\nabla^2\phi = 0. \tag{7}$$

Flows which satisfy (4)–(7) are refered to as potential flows.

After integration, (1) gives (after some algebra) the well known Bernoulli equation

$$\frac{\partial\phi}{\partial t} + \frac{\mathbf{u}\cdot\mathbf{u}}{2} + \frac{p}{\rho} + \Omega = F(t). \tag{8}$$

Here, $F(t)$ is an arbitrary function of t. It can be absorbed in the definition of ϕ and (8) can be rewritten as

$$\frac{\partial\phi}{\partial t} + \frac{\mathbf{u}\cdot\mathbf{u}}{2} + \frac{p}{\rho} + \Omega = B, \tag{9}$$

where B is a constant. For steady flows (9) reduces to

$$\frac{\mathbf{u}\cdot\mathbf{u}}{2} + \frac{p}{\rho} + \Omega = B. \tag{10}$$

3. Two-Dimensional Flows

Many interesting free surface flows can be modelled as two-dimensional flows. We then introduce Cartesian coordinates x and y with the y-axis directed vertically upwards (we reserve the letter z to denote the complex quantity $x + iy$). In the applications considered in this chapter, the body potential in (8) is due to gravity. Assuming that the acceleration of gravity g is acting in the negative y-direction, we write Ω as

$$\Omega = gy. \tag{11}$$

An example of a two-dimensional free surface is illustrated in Fig. 1. The fluid (e.g., water) is bounded below by the bottom and a circular obstacle. The flow is from left to right. The upper curve is the interface between the fluid and the atmosphere with is assumed to be characterised by a constant atmospheric pressure p_a. We refer to such an interface as a free surface. The two-dimensional configuration of Fig. 1 provides a good approximation for the three-dimensional free surface flow past a long cylinder perpendicular to the plane of the Figure (except near the ends of the cylinder). The cross section of the cylinder is the half circle shown in Fig. 1.

For two-dimensional potential flows, (4) and (6) become

$$\frac{\partial u}{\partial y} - \frac{\partial v}{\partial x} = 0 \tag{12}$$

and

$$\frac{\partial u}{\partial x} + \frac{\partial v}{\partial y} = 0. \tag{13}$$

Here, u and v are the x and y components of the velocity vector $\mathbf{u}$.

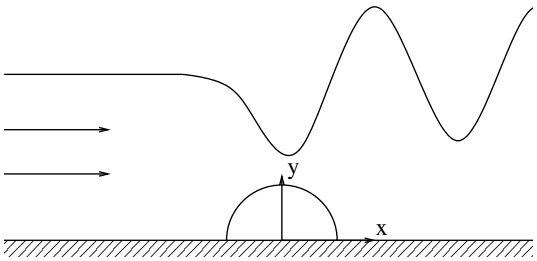

Fig. 1. Sketch of the two-dimensional free surface flow past a submerged circle

We can introduce a streamfunction ψ by noting that (13) is satisfied by writing

$$u = \frac{\partial \psi}{\partial y}, \tag{14}$$

$$v = -\frac{\partial \psi}{\partial x}. \tag{15}$$

It then follows from (12) that

$$\nabla^2 \psi = \frac{\partial^2 \psi}{\partial x^2} + \frac{\partial^2 \psi}{\partial y^2} = 0. \tag{16}$$

For two-dimensional flows, Eqs. (5) and (7) give

$$u = \frac{\partial \phi}{\partial x}, \tag{17}$$

$$v = \frac{\partial \phi}{\partial y} \tag{18}$$

and

$$\nabla^2 \phi = \frac{\partial^2 \phi}{\partial x^2} + \frac{\partial^2 \phi}{\partial y^2} = 0. \tag{19}$$

Combining (14), (15), (17) and (18) we obtain

$$\frac{\partial \phi}{\partial x} = \frac{\partial \psi}{\partial y} \tag{20}$$

$$\frac{\partial \phi}{\partial y} = -\frac{\partial \psi}{\partial x}. \tag{21}$$

Equations (20) and (21) can be recognised as the classical Cauchy-Riemann equations. They imply that the complex potential

$$f = \phi + i\psi, \tag{22}$$

is an analytic function of $z = x + iy$ in the flow domain. This result is particularly important since it implies that two-dimensional potential flows can be investigated by using the theory of analytic functions. This applies in particular to all two-dimensional potential free surface flows with or without gravity or surface tension included in the dynamic boundary condition. It does not however apply to axisymmetric and three-dimensional free surface flows. Since the derivative

of an analytic function is also an analytic function, it follows that the complex velocity

$$u - iv = \frac{\partial \phi}{\partial x} - i\frac{\partial \phi}{\partial y} = \frac{\partial \psi}{\partial y} + i\frac{\partial \psi}{\partial x} = \frac{df}{dz}, \tag{23}$$

is also an analytic functions of $z = x + iy$. The theory of analytic functions will be used intensively in the following sections to study two-dimensional free surface flows.

We now show that for steady flows the streamfunction ψ is constant along streamlines. A streamline is a line to which the velocity vectors are tangent. Let us describe a streamline in parametric form by $x = X(s)$, $y = Y(s)$, where s is the arclength. Then we have

$$-vX'(s) + uY'(s) = 0, \tag{24}$$

where the primes denote derivatives with respect to s. Using (14) and (15) we have

$$\frac{\partial \psi}{\partial x}X'(s) + \frac{\partial \psi}{\partial y}Y'(s) = \frac{d\psi}{ds} = 0, \tag{25}$$

which implies that ψ is a constant along a streamline. For steady flows the kinematic boundary condition implies that a free surface is a streamline. The streamfunction is then constant along a free surface.

An important challenge in finding solutions for flows like that of Fig. 1 is that the shape of the free surface is not known *a priori*: it has to be found as part of the solution. It is then necessary to impose an extra condition on the free surface. This is known as the dynamic boundary condition. It can be derived as follows. First we introduce the concept of surface tension by writing

$$p - p_a = \frac{T}{K}. \tag{26}$$

Here, p denotes the pressure just below the free surface, T the coefficient of surface tension (assumed to be constant) and K the curvature of the free surface. The dynamic boundary condition is then obtained by substituting (11) and (26) into (9) evaluated just below the free

surface. This yields

$$\frac{\partial \phi}{\partial t} + \frac{1}{2}(\phi_x^2 + \phi_y^2) + gy + \frac{T}{\rho}K = B. \tag{27}$$

If we denote by θ the angle between the tangent to the free surface and the horizontal, then the curvature K can be defined by

$$K = -\frac{d\theta}{ds}, \tag{28}$$

where s denotes again the arclength. In particular if the (unknown) equation of the free surface is $y = \eta(x, t)$, then

$$\tan\theta = \eta_x \quad \text{and} \quad \frac{dx}{ds} = \frac{1}{(1+\eta_x^2)^{\frac{1}{2}}}. \tag{29}$$

Using (28), (29) and the chain rule gives the formula

$$K = -\frac{\eta_{xx}}{(1+\eta_x^2)^{\frac{3}{2}}}. \tag{30}$$

4. The Mathematical Model

We shall study in details the two-dimensional free surface flow sketched in Fig. 2. The flow domain is bounded below by the horizontal wall AB and above by the inclined walls CD and DE and by the free surface EF. The fluid is assumed to be steady. We introduce Cartesian coordinates with the x-axis along the horizontal wall AB and the y-axis through the separation point E (here a separation point refers to an intersection between a free surface and a rigid wall). The angles between the walls CD and DE and the horizontal are denoted by γ_1 and γ_2 respectively.

We denote by μ the angle between the free surface and the wall at the point E. When $\mu = \pi$, the free surface is tangent to the wall at E. When $0 < \mu < \pi$, there is locally a flow inside an angle near E and the velocity at E is zero. When $\mu > \pi$, we have a flow around an angle near E and the velocity at E is infinite. We shall see in the next sections that these three cases can occur.

The configuration of Figure 2 was chosen not only because it is simple but also because it can be used to describe many properties of

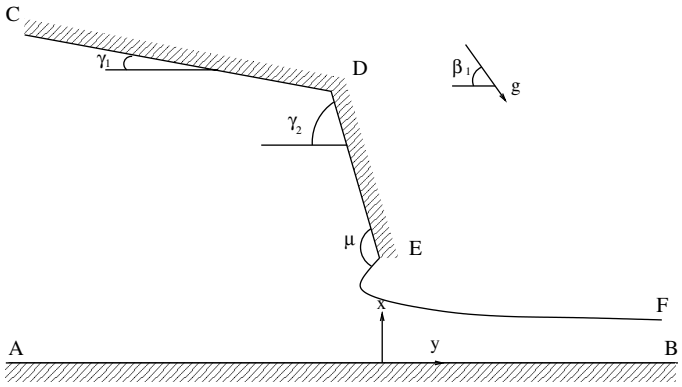

Fig. 2. A two-dimensional free surface flow bounded by the walls CD, DE and AB and the free surface EF. The separation point E is defined as the point at which the free surface EF intersects the wall DE. The points C, A, F and B are at infinite distance from E. The flow is from left to right

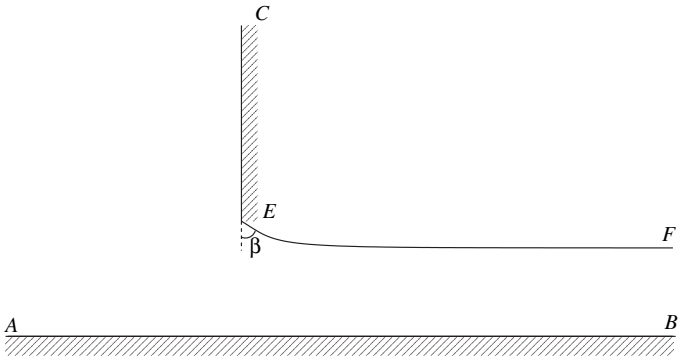

Fig. 3. Sketch of the free surface flow under a gate. The flow is from left to right

free surface flows which intersect rigid walls. These properties when understood for the flow of Figure 2 can then be used to describe locally flows with more complex geometries.

There are various interpretations of the flow of Fig. 2. The first is the flow emerging from a container bounded by the walls CD, DE and AB. When $\gamma_1 = \gamma_2 = \pi/2$, the configuration of Fig. 2 models the flow under a gate (see Fig. 3). Here the point D is irrelevant and was omitted from the Fig. 3.

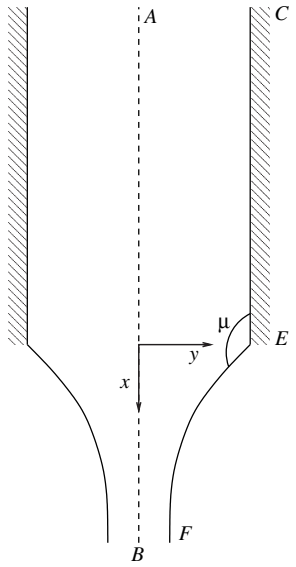

Fig. 4. The free surface flow emerging from a nozzle

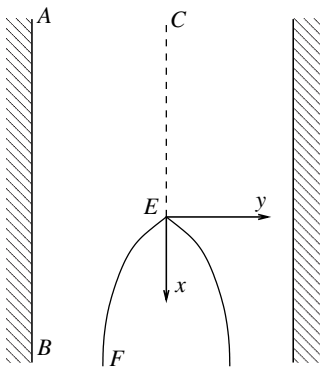

Fig. 5. A "bubble" rising in a tube, viewed in a frame of reference moving with bubble. Physical bubbles are characterised by a continuous slope at the apex

Further particular cases of Fig. 2, which model bubbles rising in a fluid and jets falling from a nozzle are illustrated in Figs. 4 and 5.

As mentioned in the introduction we will proceed with problems of increasing complexity. Section 5 is devoted to free surface flows with $g = 0$ and $T = 0$. Such flows are called free streamline flows

and the corresponding free surfaces, free streamlines. In Sec. 6 we will study the effect of surface tension ($T \neq 0$, $g = 0$). In Sec. 7 we will examine the effect of gravity ($T = 0$, $g \neq 0$). The combined effects of gravity and surface tension ($T \neq 0$, $g \neq 0$) are considered in Sec. 8.

5. Free Streamline Flows: $g = 0$, $T = 0$

5.1. *Forced separation*

We consider the flow configuration of Fig. 2. The effects of gravity and surface tension are neglected ($T = 0$, $g = 0$). We refer to this problem as one of forced separation because the free surface is "forced" to separate at the point E where the wall DE terminates. Following the notations of Sec. 3 we introduce the complex potential function $f = \phi + i\psi$ and the complex velocity $u - iv$.

The wall AB is a streamline along which we choose $\psi = 0$. The walls CD and DE and the free surface EF define another streamline along which the constant value of ψ is denoted by Q. We also choose $\phi = 0$ at the separation point E. These two choices ($\psi = 0$ on AB and $\phi = 0$ at E) can be made without loss of generality because ϕ and ψ are defined up to arbitrary additive constants. Bernoulli's equation (10) with $\Omega = 0$ yields

$$\frac{1}{2}(u^2 + v^2) + \frac{p}{\rho} = \text{constant} \tag{31}$$

everywhere in the fluid. The free surface EF separates the fluid from the atmosphere which is assumed to be characterised by a constant pressure p_a. In the abscence of surface tension, the pressure is continuous across the free surface (see (26)). Therefore $p = p_a$ on the free surface. It follows from (31) that

$$u^2 + v^2 = U^2 \quad \text{on EF} \tag{32}$$

where U is a constant.

A significant simplification in the formulation of the problem is obtained by using ϕ and ψ as independent variables. This choice was

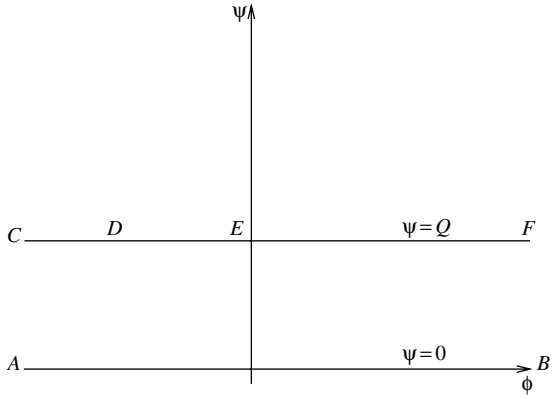

Fig. 6. The flow configuration of Fig. 2 in the complex potential plane $f = \phi + i\psi$

used before by many investigators (see Vanden-Broeck [5] for references). We shall use it extensively in our studies of gravity capillary free surface flows. The simplification comes from the fact that the flow domain is mapped into the strip $0 < \psi < Q$ shown in Figure 6.

The free surface EF (whose position was unknown in the physical plane $z = x + iy$ of Fig. 2) is now part of the known boundary $\psi = Q$ in the $f = \phi + i\psi$-plane. Since $u - iv$ is an analytic function of z and z is an analytic function of f (the inverse of an analytic function is also an analytic function), $u - iv$ is an analytic function of f.

A remarkable result is that many free streanline problems can be solved in closed form (see Birkhoff and Zarantonello[3] and Gurevich[4]). These exact solutions are obtained by using conformal mappings and several methods have been developed to calculate them. The method we chose to describe, uses a mapping of the flow domain into the unit circle. It was chosen because it yields naturally to the series truncation methods used in Secs. 6, 7 and 8 to solve numerically problems with gravity and surface tension included.

In the absence of gravity and surface tension, the flow approaches a uniform stream of constant depth H as $x \to \infty$. It follows from the dynamic boundary condition (32) that this uniform stream is characterised by a constant velocity U. Since $\psi = 0$ on AB and $\psi = Q$ on EF, $H = Q/U$. We introduce dimensionless variables

by using U as the reference velocity and H as the reference length. Therefore $\psi = 1$ on the walls CD and DE and on the free surface EF. The dynamic boundary condition (32) becomes

$$u^2 + v^2 = 1 \quad \text{on } EF. \tag{33}$$

We define the logarithmic hodograph variable $\tau - i\theta$ by the relation

$$u - iv = e^{\tau - i\theta}. \tag{34}$$

The function $\tau - i\theta$ has some interesting properties. Firstly the quantity $\tau = \frac{1}{2}\ln(u^2 + v^2)$ is constant along free streamlines (see (32)). Secondly θ can be interpreted as the angle between the vector velocity and the horizontal. Thirdly (34) leads, for steady flows, to a very simple formula for the curvature of a streamline. This formula can be derived as follows. Since the vector velocity is tangent to streamlines, θ is the angle between the tangent to a streamline and the horizontal. The curvature K of a streamline is then given by (28). Using the chain rule we rewrite (28) as

$$K = -\frac{\partial\theta}{\partial\phi}\frac{\partial\phi}{\partial s} - \frac{\partial\theta}{\partial\psi}\frac{\partial\psi}{\partial s}. \tag{35}$$

Along a streamline ψ is constant and therefore

$$\frac{\partial\psi}{\partial s} = 0 \quad \text{and} \quad \frac{\partial\phi}{\partial s} = e^{\tau}. \tag{36}$$

Substituting (36) into (35) yields the simple formula

$$K = -e^{\tau}\frac{\partial\theta}{\partial\phi}. \tag{37}$$

We map the strip of Figure 6 into the unit circle in the t-plane by the conformal mapping

$$e^{-\pi f} = \frac{(1-t)^2}{4t}. \tag{38}$$

The flow configuration in the t-plane is shown in Fig. 7. It can easily be checked that the points A and C are mapped into $t = 0$ and that the points B and F are mapped into $t = 1$. The value of t

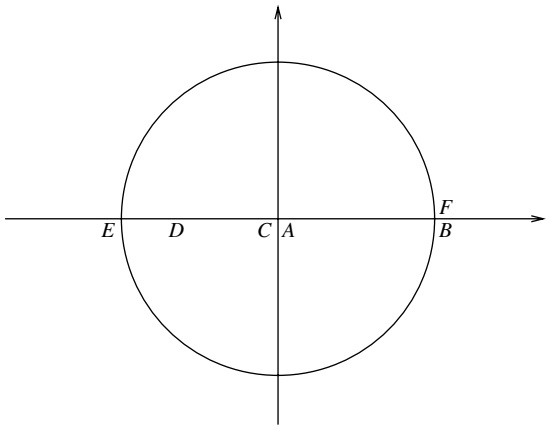

Fig. 7. The flow configuration of Fig. 6 in the complex t-plane. Here we sketch values of the imaginary value of t versus the real part of t

at the point D is denoted by $t = d$. The free surface EF is mapped onto the portion

$$t = e^{i\sigma}, \quad 0 < \sigma < \pi \tag{39}$$

of the unit circle. This can easily be shown by noting that a substitution of (39) into (38) gives after some algebra

$$\phi = -\frac{1}{\pi} \ln \sin^2 \frac{\sigma}{2}, \quad \psi = 1. \tag{40}$$

As σ varies from 0 to π, ϕ varies from ∞ to 0, so that (39) is the image of the free surface in the t-plane.

One might attempt to represent the complex velocity $w = u - iv$ by the series

$$w = \sum_{n=0}^{\infty} a_n t^n. \tag{41}$$

However the series will not converge inside the unit circle $|t| \leq 1$, because singularities can be expected at the corner D and as $x \to -\infty$ (i.e., at $t = 0$). We can however generalise the representation (41) by writing

$$w = G(t) \sum_{n=0}^{\infty} a_n t^n \tag{42}$$

where the function $G(t)$ contains all the singularities of w. As we shall see in Secs. 6–8 this type of series representation enables the accurate calculation of many free surface flows with gravity and surface tension included. For the present problem we require $G(t)$ to behave like w as $t \to 0$ and as $t \to d$. Here d is the value of t at the point D in Fig. 7. We can then expect the series in (42) to converge for $|t| \leq 1$.

To construct $G(t)$, we find the asymptotic behaviour of w near the singularities by performing local asymptotic analysis near D and as $x \to -\infty$.

The flow near D is a flow inside a corner. It can be shown that the general solution for a flow in a corner γ is

$$z \approx A f^{\frac{\gamma}{\pi}}, \tag{43}$$

where A is a constant. It follows from (43) that

$$w \approx \frac{\pi}{A\gamma} f^{1-\frac{\gamma}{\pi}}. \tag{44}$$

When $\gamma < \pi$, the flow is inside at the angle and (44) implies that the velocity at the apex is zero. When $\gamma > \pi$, the flow is around the angle and (44) implies that the velocity at the apex is infinite.

For the flow of Figure 2, $\gamma = \pi - \gamma_2 + \gamma_1$ and (44) implies

$$w = (f - \phi_D - i)^{\left(\frac{\gamma_2 - \gamma_1}{\pi}\right)} \quad \text{as } f \to \phi_D + i \tag{45}$$

where ϕ_D is the value of ϕ at the point D. Using (38), yields

$$f - \phi_D - i \approx t - d \quad \text{as} \quad f \to \phi_D + i. \tag{46}$$

Combining (45) and (46) gives

$$w \approx (t - d)^{\left(\frac{\gamma_2 - \gamma_1}{\pi}\right)} \quad \text{as } t \to d. \tag{47}$$

This concludes our local analysis near the point D.

As $x \to -\infty$, the flow behaves like the flow due to a sink at $x = y = 0$. Therefore

$$f \approx -B \ln z \quad \text{as} \quad x \to -\infty, \tag{48}$$

where B is a positive constant. Differentiating (48) with respect to z gives

$$w = \frac{df}{dz} = -\frac{B}{z}. \tag{49}$$

Since the flux of the fluid coming from $-\infty$ is 1 and the angle between the walls CD and AB is γ_1, we have

$$B = \frac{1}{\gamma_1}. \tag{50}$$

Eliminating z between (48) and (49) gives

$$w = O[e^{\gamma_1 f}] \quad \text{as } f \to -\infty. \tag{51}$$

Relation (38) implies

$$e^{\pi f} = O(t) \quad \text{as} \quad f \to -\infty. \tag{52}$$

Therefore (51) and (52) give

$$w = O(t^{\frac{\gamma_1}{\pi}}) \quad \text{as} \quad t \to 0. \tag{53}$$

Combining (47) and (53), we can choose

$$G(t) = (t-d)^{\frac{(\gamma_2-\gamma_1)}{\pi}} t^{\frac{\gamma_1}{\pi}} \tag{54}$$

and write (42) as

$$w = (t-d)^{(\gamma_2-\gamma_1)/\pi} t^{\gamma_1/\pi} \sum_{n=0}^{\infty} a_n t^n. \tag{55}$$

There are of course many other possible choices for $G(t)$. For example, $G(t)$ can be multiplied by any function analytic in $|t| \leq 1$.

We now need to determine the coefficients a_n in (55) so that the dynamic boundary condition (33) is satisfied. This can be done numerically by truncating the infinite series in (55) after N terms and finding the coefficients a_n, $n = 0 \ldots, N-1$ by collocation. This is the approach we will use when solving problems with the effects of gravity or surface tension included in the dynamic boundary condition. However it can checked that the problem has the exact solution

$$w = \left[\frac{t-d}{1-td}\right]^{\frac{(\gamma_2-\gamma_1)}{\pi}} t^{\frac{\gamma_1}{\pi}}. \tag{56}$$

It then follows from (55) that

$$\sum_{n=1}^{\infty} a_n t^n = \left[\frac{1}{1-td}\right]^{\frac{(\gamma_2-\gamma_1)}{\pi}}. \tag{57}$$

The existence of an exact solution follows from the general theory of free streamline flows. This theory was developed by Kirchhoff and Helmoltz (see Birkhoff and Zarantonello[3] and Gurewich[4] for details).

The free surface profile is obtained by setting $\psi = 1$ in (56), calculating x_ϕ and y_ϕ from the identity

$$x_\phi + iy_\phi = \frac{1}{w} \tag{58}$$

and integrating with respect to ϕ.

As an example let us assume that $\gamma_1 = \gamma_2 = \pi/2$ (see Figure 3). Then (56) reduces to

$$w = t^{\frac{1}{2}} \tag{59}$$

and (39), (58) and (59) yield

$$x_\phi + iy_\phi = e^{-\frac{i\sigma}{2}} \quad \text{on} \quad 0 < \sigma < \pi \tag{60}$$

on the free surface EF. Differentiating (40) with respect to σ and applying the chain rule to (60) gives

$$x_\sigma + iy_\sigma = -\frac{1}{\pi}\text{cotan}\frac{\sigma}{2}e^{-\frac{i\sigma}{2}}. \tag{61}$$

Integrating (61) gives the free profile in parametric form. It is shown in Fig. 8.

5.2. *Free separation*

In Figs. 2 and 3 the free surface is forced to separate from the rigid wall DE at E because the wall DE terminates at E. We refer to this situation as forced separation. On the other hand, if the wall DE is replaced by a smooth curve then the point of separation E can be in principle any point on the smooth curve. We refer to this situation as free separation.

A typical example of free separation is the cavitating flow past a circle (see Fig. 9).

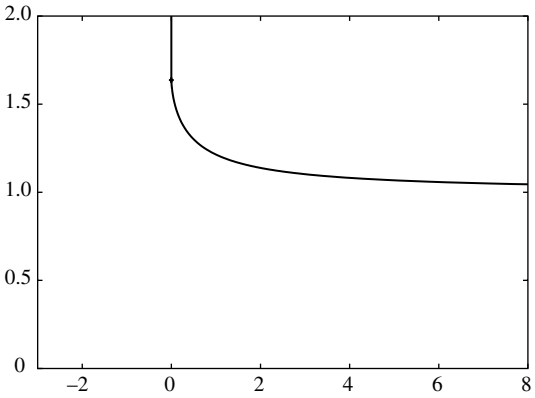

Fig. 8. Computed free surface profile (values of y versus x) for the flow configuration of Figure 3. The position of the separation point E is indicated by a small horizontal line. The vertical scale has been exagerated to show clearly the free surface profile. The bottom is on $y = 0$

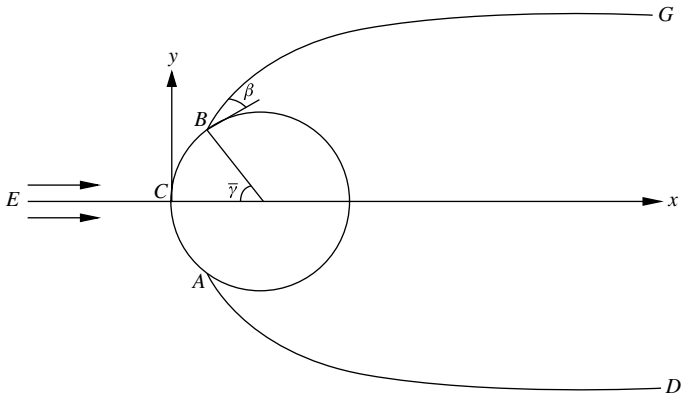

Fig. 9. The cavitating flow past a circle in an unbounded fluid domain. When the surface tension T is equal to zero the free surfaces leave the circle tangentially and $\beta = 0$. When $T \neq 0$ the angle β can be different from zero

The cavity is bounded by the two free surfaces BG and AD. It is characterised by a constant pressure p_a and it is open as $x \to \infty$. The position of the separation points A and B is characterised by the angle $\bar{\gamma}$. The angle between the free surfaces and the circle at the separation points B and A is denoted by β. Since we assumed in

this section that $g = 0$ and $T = 0$, we have $\beta = 0$. We will see in the next sections that β can be different from zero when $T \neq 0$. There no exact solution for the flow of Fig. 9 because the rigid boundaries are not polygonal. However solutions can be calculated numerically by series truncation. Details can be found in Vanden-Broeck.[5] The results show that the value of the angle $\bar{\gamma}$ does not come as part of the solution. In other words there is a flow for each value of $\bar{\gamma}$. A natural question is: which value of $\bar{\gamma}$ will be selected in an experiment? One way to select a solution is to impose an extra condition known as the Brioullin condition (see Birkhoff and Zarantonello[3] and Gurewich[4] for details). It leads to the values

$$\gamma^* \approx 55^0. \tag{62}$$

As we shall see in Sec. 6.2 an alternative way to achieve this selection is to introduce the surface tension T in the problem and then to take the limit $T \to 0$.

6. Pure Capillary Free Surface Flows: $g = 0$, $T \neq 0$

6.1. *Forced separation*

In this section we will investigate the effects of the surface tension T on the free streamline solutions of Sec. 5. We show that the limit $T \to 0$ is singular. When $T \neq 0$ discontinuities can appear at the separation points. In particular vales of $\mu \neq \pi$ and $\beta \neq 0$ can occur in Figures 2 and 3.

We can calculate nonlinear solutions for the flow configuration of Fig. 2 by modifying appropriately the series representation (55) to accomodate the singularity at $t = -1$. The flow near $t = -1$ is a flow in an angle μ. Using (44) we obtain

$$w \sim f^{1-\frac{\mu}{\pi}} \quad \text{as } \phi \to 0. \tag{63}$$

Using (38) we have

$$w \sim (t+1)^{2-\frac{2\mu}{\pi}} \quad \text{as} \quad t \to -1. \tag{64}$$

Therefore

$$w = (t-d)^{\frac{(\gamma_2-\gamma_1)}{\pi}} t^{\frac{\gamma_1}{\pi}} (t+1)^{2-\frac{2\mu}{\pi}} \sum_{n=0}^{\infty} a_n t^n \tag{65}$$

is the appropriate generalisation of (55) when surface tension is included.

We present explicit calculations in the particular case $\gamma_1 = \gamma_2 = \pi/2$. In other words we consider the flow configuration of Figure 3. The expression (65) becomes

$$w = t^{\frac{1}{2}}(t+1)^{-\frac{2\beta}{\pi}} \sum_{n=0}^{\infty} a_n t^n, \tag{66}$$

where β is defined in Fig. 3.

The dynamic boundary condition is given in dimensionless variables ($U = 1$, $H = 1$) by

$$\frac{1}{2}(u^2 + v^2) + \frac{2}{\alpha_v} K = \text{constant}, \tag{67}$$

where α_v is defined by

$$\alpha_v = \frac{2\rho U^2 H}{T}. \tag{68}$$

Since $u^2 + v^2 \to 1$ and $K \to 0$ as $\phi \to \infty$, the constant on the right-hand side of (67) is equal to $1/2$.

We truncate the infinite series in (66) after N terms. We calculate the coefficients a_n, $n = 0, \ldots, N-1$ and β by satisfying (67) (with K rewritten in terms of u and v by using (37)) at the $N+1$ equally spaced mesh points

$$\sigma_I = \frac{\pi}{N+1}(I - \frac{1}{2}) \quad I = 1, \ldots, N+1. \tag{69}$$

This leads a system of $N+1$ equations with $N+1$ unknowns which is solved by Newton's method.

Typical free surface profiles are shown in 10. For $\alpha_v = \infty$, the free surface profile reduces to the free streamline solution of Fig. 8. As $\alpha_v \to 0$, the free surface profile approaches the horizontal line $y = 1$. This is consistent with the fact that the dynamic boundary condition (67) predicts that the curvature of the free surface tends to zero as $\alpha_v \to 0$ (the line $y = 1$ has zero curvature).

Numerical values of β versus α_v are shown in Figure 11.

As α_v varies from 0 to ∞, β varies continuously from $\pi/2$ to 0.

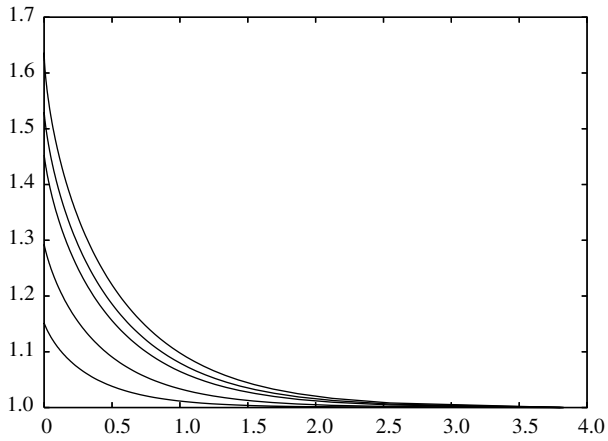

Fig. 10. Computed free surface profiles (values of y versus x) for the flow configuration of Figure 3. The profiles from top to bottom correspond to $\alpha_v = \infty$, $\alpha_v = 50$, $\alpha_v = 25$, $\alpha_v = 10$ and $\alpha_v = 5$. The bottom is on $y = 0$

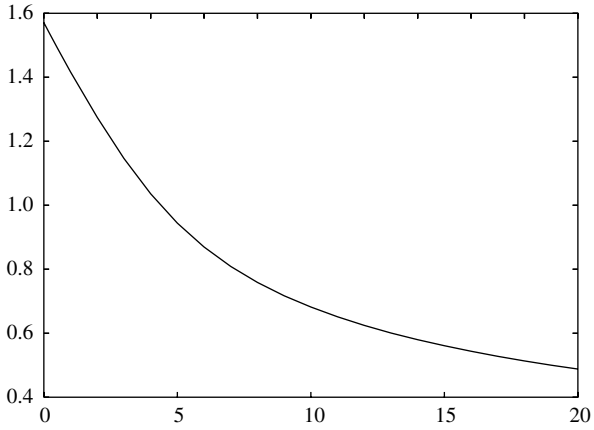

Fig. 11. Values of the angle β between the free surface and the wall at the separation point E (see Figure 3) versus α_v

6.2. *Free separation*

We now consider the open cavity model of Fig. 9 with the effect of the surface tension T included in the dynamic boundary condition. The results presented in the previous section suggests that the angle

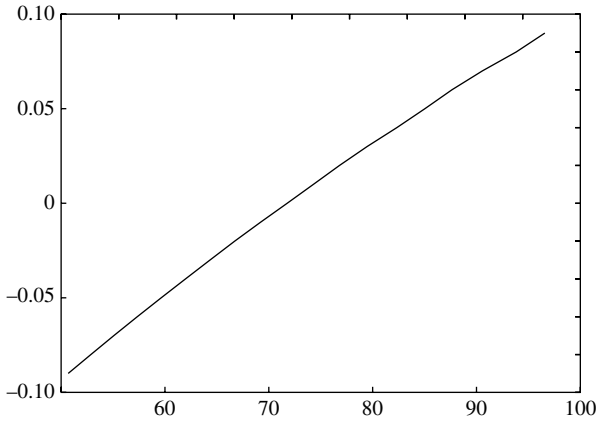

Fig. 12. Values of β/π versus $\bar{\gamma}$ for $\bar{\alpha} = 1$

β in Fig. 9 will be different from zero when $T \neq 0$. This is confirmed by solving the problem numerically by using the series truncation procedure outlined in Sec. 5.1. The reader is referred to Vanden-Broeck[5] for details. We present in Fig. 12 values β/π versus $\bar{\gamma}$ for $\bar{\alpha} = 1$. Here, $\bar{\alpha}$ is defined by

$$\bar{\alpha} = \frac{\rho U^2 R}{T}, \tag{70}$$

where R is the radius of the circle.

Figure 12 illustrates the fact that for each value $\bar{\alpha}$ (i.e., for each value of T) there is only one value of $\bar{\gamma}$ for which $\beta = 0$. We describe these particular values of $\bar{\gamma}$ by the function $\bar{\gamma} = g(\bar{\alpha})$. This means that for $\bar{\gamma} = g(\bar{\alpha})$ the free surface leaves the circle tangentially. The numerical calculations show that

$$g(\bar{\alpha}) \to \gamma^* \quad \alpha \to \infty \tag{71}$$

where γ^* is defined in (62).

Therefore a unique solution is obtained in the limit as T tends to zero. This shows that the solution satisfying the Brioullin condition can be selected by including surface tension in the problem and then taking the limit $T \to 0$.

7. Pure Gravity Free Surface Flows: $g \neq 0$, $T = 0$

For pure gravity flows, the angles μ and β in Figs. 2 and 3 come also as part of the solution. However they are restricted to a few values. For example for the flow of Fig. 4, μ can only take one of the three values $\pi/2$, $2\pi/3$ and π. Here (and in the remaining part of this chapter) we assume that gravity is acting vertically downwards. Numerical solutions can be obtained by adapting appropriately the series truncation method of Secs. 5 and 6. Details can be found in Vanden-Broeck.[5]

We present results for the flow sketched in Figs. 4 and 5. We first note that these two flows are equivalent by symmetry: the free surfaces EF in Figs. 4 and 5 are identical. We chose to describe the results by refering to Fig. 5. Following the notations in Vanden-Broeck,[5] we introduce the Froude number

$$F = \frac{U}{\sqrt{gh}} \tag{72}$$

and the parameter

$$\nu = 2\frac{\pi - \mu}{\pi}, \tag{73}$$

where h is the distance between the two vertical walls in Figure 5.

Figure 13 shows numerical values of ν versus F. These results imply

$$\nu = 1, \quad \mu = \frac{\pi}{2} \quad \text{for } 0 < F < F_c \tag{74}$$

$$\nu = \frac{2}{3}, \quad \mu = \frac{2\pi}{3} \quad \text{for } F = F_c \tag{75}$$

$$\nu = 0, \quad \mu = \pi \quad \text{for } F > F_c \tag{76}$$

where

$$F_c \approx 0.3578. \tag{77}$$

Physically relevant bubbles should have a continuous slope at their apex. This occurs for all values of $0 < F < F_c$. Experiments show that bubbles are only observed for

$$F_e \approx 0.25. \tag{78}$$

This value is clearly in the interval $0 < F < F_c$. However we do not have at this stage any criterion to select this particular solution. The

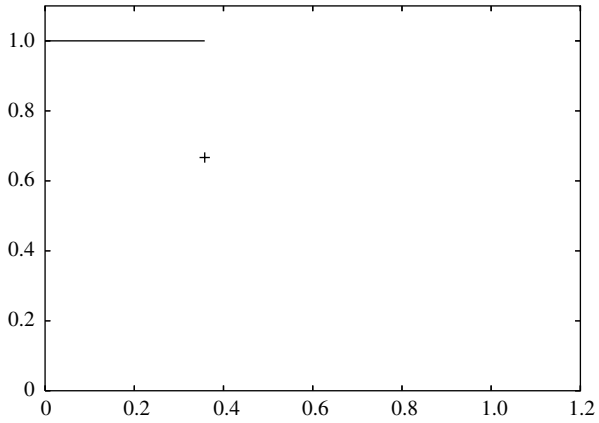

Fig. 13. Values of ν versus F when $T = 0$

selection will again be achieved in the next section by introducing the surface tension T and taking the limit $T \to 0$.

8. Gravity-Capillary Free Surface Flows: $g \neq 0$, $T \neq 0$

When $g \neq 0$ and $T \neq 0$, the angles μ and β are again found as part of the solution. However they can take in principle any values as it was the case in Sec. 6 where $T \neq 0$ and $g = 0$. This is to be contrasted to the case $g \neq 0$ and $T = 0$ of Sec. 7 where the angle μ was restricted to three values. We can therefore expect the limit $T \to 0$ to be a singular limit.

We present explicit results for the flow of Fig. 5. We first introduce the parameter

$$\alpha^* = \frac{\rho U^2 h}{T}. \tag{79}$$

Values of ν versus F for $\alpha^* = 10$ are presented in Figs. 14 and 15. These results show that there is a countably infinite set of values of F for which $\nu = 1$. This is to be contrasted to the case $T = 0$ (i.e., $\alpha^* = \infty$) for which $\nu = 1$ for all values $0 < F < F_c$. More interestingly it can be shown that this discrete set of values coalesce

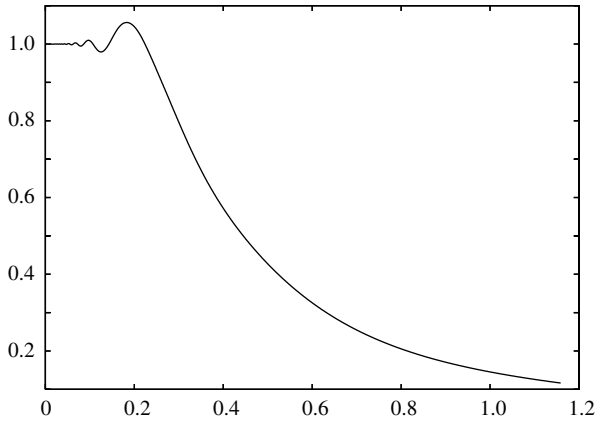

Fig. 14. Values of ν versus F for $\alpha^* = 10$

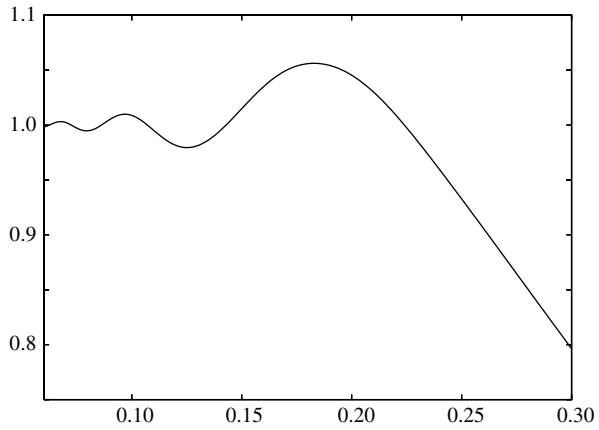

Fig. 15. Enlargement of Figure 14 showing clearly the oscillations

to a unique value

$$F^{**} \approx 0.23 \quad \text{as } T \to 0 \tag{80}$$

(see Vanden-Broeck [5]). This is illustrated in Fig. 16 where we plot the value F_1^* of the largest value of the discrete set versus $1/\alpha^*$. As $T \to 0$ (i.e., as $1/\alpha^* \to 0$), $F_1 \to F^{**}$ in agreement with (80). The value of F^{**} is close to the experimental value (78). This shows that the physically relevant bubble is selected by including the surface tension T and taking the limit $T \to 0$.

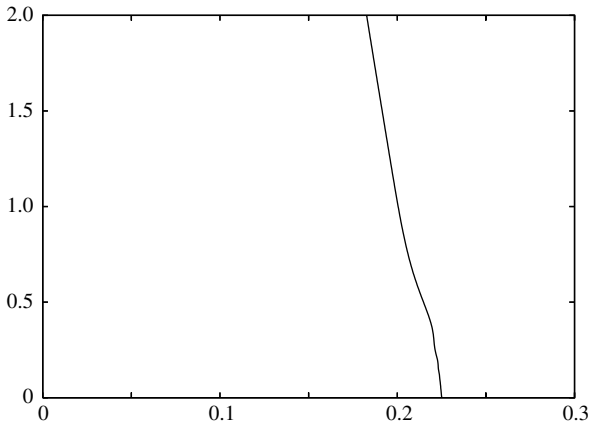

Fig. 16. Values of $1/\alpha^*$ versus F_1^*. As $1/\alpha^* \to 0$, $F_1^* \to F^{**} \approx 0.23$

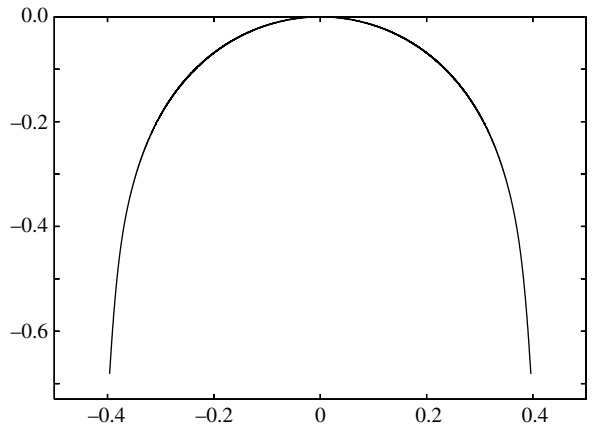

Fig. 17. The selected bubble

The selected profile is shown in Fig. 17.

9. Some Exercises

(1) Derive equation (38). Hint: first map the strip of Figure (6) onto to the lower half-plane.
(2) Derive equation (43).

(3) Use the result in (1) to derive (44).
(4) Define the contraction ratio y_F/y_E in Fig. 3. Consider now the flow in Fig. 8. Show that the contraction ratio is $\frac{\pi}{2+\pi}$.
(5) Derive the appropriate generalisation of (66) for the flow of Fig. 4. Assume $T = 0$ and $g \neq 0$.

10. Conclusions

We have studied some nonlinear gravity-capillary free surface flows. Special attention was devoted to problems for which the free surfaces intersect rigid surfaces. We hope to have convinced the reader of the mathematical beauty of these flows. Due to the space limitation we restricted our attention to steady waveless potential flows. Further extensions to rotational flows, free surface flows with waves, time dependent problems and three-dimensional flows can be found in Vanden-Broeck[5] and in the references cited there.

References

1. D. J. Acheson, *Elementary Fluid Dynamics*. Oxford University Press (1990).
2. G. K. Batchelor, *Fluid Dynamics*. Cambridge University Press, p. 615.
3. G. Birkhoff and E. Zarantonello, *Jets, Wakes and Cavities*. Academic Press (1957).
4. M. Gurevich, *Theory of Jets and Ideal Fluids*. Academic Press (1965).
5. J.-M. Vanden-Broeck, *Gravity-Capillary Free Surface Flows*. Cambridge University Press.